

Predicting hepatocellular carcinoma early recurrence after ablation based on magnetic resonance imaging radiomics nomogram

Xiaozhen Yang, MS^{a,b}, Chunwang Yuan, MD^b, Yinghua Zhang, MS^b, Kang Li, MD^c, Zhenchang Wang, MD^{a,*} 

Abstract

Background: The aim of this study is to investigate a model for predicting the early recurrence of hepatocellular carcinoma (HCC) after ablation.

Methods: A total of 181 patients with HCC after ablation (train group was 119 cases; validation group was 62 cases) were enrolled. The cases of early recurrence in the set of train and validation were 63 and 31, respectively. Radiomics features were extracted from the enhanced magnetic resonance imaging scanning, including pre-contrast injection, arterial phase, late arterial phase, portal venous phase, and delayed phase. The least absolute shrinkage and selection operator cox proportional hazards regression after univariate and multivariate analysis was used to screen radiomics features and build integrated models. The nomograms predicting recurrence and survival of patients of HCC after ablation were established based on the clinical, imaging, and radiomics features. The area under the curve (AUC) of the receiver operating characteristic curve and C-index for the train and validation group was used to evaluate model efficacy.

Results: Four radiomics features were selected out of 34 texture features to formulate the rad-score. Multivariate analyses suggested that the rad-score, number of lesions, integrity of the capsule, pathological type, and alpha-fetoprotein were independent influencing factors. The AUC of predicting early recurrence at 1, 2, and 3 years in the train group was 0.79 (95% CI: 0.72–0.88), 0.72 (95% CI: 0.63–0.82), and 0.71 (95% CI: 0.61–0.83), respectively. The AUC of predicting early recurrence at 1, 2, and 3 years in the validation group was 0.72 (95% CI: 0.58–0.84), 0.61 (95% CI: 0.45–0.78) and 0.64 (95% CI: 0.40–0.87).

Conclusion: The model for early recurrence of HCC after ablation based on the clinical, imaging, and radiomics features presented good predictive performance. This may facilitate the early treatment of patients.

Abbreviations: 3D = 3-dimensional, AFP = alpha-fetoprotein, AUC = area under the curve, CT = computer tomography, HCC = hepatocellular carcinoma, LASSO = least absolute shrinkage and selection operator, MRI = magnetic resonance imaging, VOI = volume of interest.

Keywords: ablation, nomogram, predicting hepatocellular carcinoma, predictive model, prognosis

1. Introduction

Hepatocellular carcinoma (HCC) was the fifth most common cancer and the second most frequent cause of cancer-related death globally.^[1] The recurrence of HCC reduces the overall survival of the patients. Recognition of early recurrence helps with the timely treatment and in developing a follow-up strategy. Shortening follow-up intervals and multidisciplinary tactics should be performed in cases of early recurrence. In previous studies, several indicators such as microvascular invasion, texture analysis, and Ki67 expression had been studied.^[2–4] However, recognition of early

recurrence is still a clinical challenge. Until now, there was no effective strategy that predicts early recurrence for HCC patients after ablation.

Several indicators may indicate the prognosis for hepatectomy, such as tumor differentiation, level of alpha-fetoprotein (AFP), clinical stages and status, hepatitis type, Child-Pugh class, microvascular invasion and so on.^[5,6] In addition, the features of tumor imaging probably present heterogeneity. Some imaging features were known as independent factors for recurrence, such as tumor margin, and peritumoral hypointensity.^[7,8] However, no quantification measure was reliable for the prediction of HCC recurrence within 1 year.

The authors have no funding and conflicts of interest to disclose.

The datasets generated during and/or analyzed during the current study are available from the corresponding author on reasonable request.

This study was approved by the Ethics Committee of Beijing Youan Hospital, and the informed consent requirement was waived.

^a Department of Radiology, Beijing Friendship Hospital, Capital Medical University, Beijing, China, ^b Department of Center of Interventional Oncology and Liver Diseases, Beijing Youan Hospital, Capital Medical University, Beijing, China, ^c Biomedical Information Center, Beijing You'an Hospital, Capital Medical University, Beijing, China.

* Correspondence: Zhenchang Wang, Department of Radiology, Beijing Friendship Hospital, Capital Medical University, No. 95, Yong An Road, Xicheng District, Beijing 100050, China (e-mail: wangzhenchang6@126.com).

Copyright © 2022 the Author(s). Published by Wolters Kluwer Health, Inc. This is an open-access article distributed under the terms of the Creative Commons Attribution-Non Commercial License 4.0 (CCBY-NC), where it is permissible to download, share, remix, transform, and buildup the work provided it is properly cited. The work cannot be used commercially without permission from the journal.

How to cite this article: Yang X, Yuan C, Zhang Y, Li K, Wang Z. Predicting hepatocellular carcinoma early recurrence after ablation based on magnetic resonance imaging radiomics nomogram. *Medicine* 2022;101:52(e32584).

Received: 11 November 2022 / Received in final form: 13 December 2022 / Accepted: 15 December 2022

<http://dx.doi.org/10.1097/MD.00000000000032584>

Radiomics is a comprehensive method used to analyze medical images which was first proposed in 2012.^[9,10] Essential steps such as data acquisition and preprocessing, feature extraction, and modeling are involved in radiomics.^[9] The radiomic features highlighted the prediction of HCC early recurrence by quantification signatures.^[11,12] Until now, there were few studies around radiomics and ablation therapy. However, results of the studies proved that the texture analysis was reliable for predicting the prognostic of HCC after hepatectomy.^[11,12] Although there was no consensus, the radiomics feature carried a lot of weight for directions of oncology, such as predicting recurrence, outcome, survival, and differential diagnosis.^[13–20] Meanwhile, almost all kinds of modalities could be utilized for analysis, such as computer tomography (CT), magnetic resonance imaging (MRI), PET-CT and US.^[21–23]

Previous studies had proved that the texture analysis was reliable for predicting the prognostic of HCC after hepatectomy.^[11,12] However, there were few reports on the prediction model of early recurrence of HCC after ablation. In the present study, we established a model for predicting the early recurrence of HCC after ablation. This exploration probably provides new evidence and conclusions for personalized medicine, and layer patients of high risk with close follow-up or supplementary treatment.

2. Materials and methods

2.1. Patients

This study was approved by the Ethics Committee of Beijing Youan Hospital, and the informed consent requirement was waived. A total of 181 patients of HCC after ablation were recruited. The cases were confirmed pathologically in Beijing Youan Hospital, from November 2012 to April 2018, and had undergone ablation. The cases of male and female were 146 and 35, respectively. The cases were separated into 2 groups (train and validation) randomly by computer generated numbers. There were 119 and 62 cases in the groups of train and validation. The cases of early recurrence in the set of train and validation were 63 and 31, respectively.

2.1.1. Inclusion criteria.

- (1) The patient was diagnosed by pathology.
- (2) Preablation enhanced MRI image was available.
- (3) Cases with complete clinical data. Early recurrence was defined as enhanced CT, MRI or DSA showed new lesion in the remnant liver or outside the liver within 1 year after ablation.

Follow up: the patient took examination and test every 3 months. All the values of alanine transaminase, aspartate transaminase, platelet, AFP, overall survival, recurrence time, age, gender, tumor node metastasis stage, maximum tumor diameter, and pathological type were recorded. Image characteristics of the lesion were recorded, such as lesion number, artery supply, capsule, margin, necrosis, uniform enhancement.

2.2. MRI examination

The patients underwent enhanced MRI scanning, including pre-contrast injection, arterial phase, late arterial phase, portal venous phase, delayed phase. The time was 12 to 15 seconds, 26 to 29 seconds, 180 seconds, and 300 seconds. The scanning sequence were axial T1WI, axial T2WI, axial inverse phase imaging and multiphase enhanced T1WI, T2WI coronal plane and DWI transverse plane. Scanning range from diaphragm roof to complete liver, gallbladder, pancreas and spleen. The inspection machine was a Siemens Tro Tim 3.0T superconducting MRI system, and the phase coil was a SENSE body coil.

Plain scan was performed using axial Turbo-FLASH T1WI (TR: 1400 seconds; TE: 2.46 ms; slice thickness: 6 mm; slice spacing: 1.8 mm; FOV: 380; excitation times 1; matrix 320 × 256), axial TSE T2WI (TR: 1500 ms; TE: 92 ms; layer thickness 6 mm; layer spacing 1.8 mm; FOV: 380 mm; excitation times: 1; matrix: 320 × 256). Enhanced scanning was performed using 3-dimensional (3D)-VIEB (TR: 3.5 ms; TE: 1.28 ms; slice thickness: 3 mm; slice distance: 0.6 mm; FOV: 380 mm; excitation times: 1; matrix: 320 × 256). Gd-DTPA was used as contrast agent for enhanced scanning, with a dose of 0.2 to 0.3 mL/kg and a flow rate of 2.5 mL/s. All patients were with an empty stomach before examination.

2.3. Image segmentation

The digital imaging and communications in medicine format image was down load from PACS in Youan Hospital, Beijing. The ITK-SNAP software was used to outline the lesions. The enhanced MRI imaging (T1W, T2W, late arterial phase, portal-venous phase, delayed portal phase) of tumors were delineated manually slice by slice. The radiologists delineated the lesion was blind of the follow-up outcome of the cases. Radiologists manually delineated the region of interest along the edge of the lesion, layer by layer. The volume of interest (VOI) of the lesion was automatically generated by the computer. If there were 3 lesions, we chose the biggest 1. LIFEx 4.90 software extracted radiomics features from the imaging. The end time of the study was 31st December of 2019.

2.4. Radiomics features and modeling

We used LIFEx 4.90 software to extract radiomics features after delineating the VOI of each lesion, totally 200 for each patient. The Student's *t* test and Mann-Whitney *U* test were used for screening the potential relative features by *R* studio. Among the 200 radiomics features, 34 radiomics features were used for analyzed. The mean value was filled in the absent 1. Four radiomics features were left for the least absolute shrinkage and selection operator (LASSO) cox proportional hazards regression after univariate and multivariate analysis. We established an integration predictive model, including radiomics features, clinical and imaging semantic features. The area under the curve of receiver operating characteristic curve for train and validation group was used to evaluate model efficacy.

2.5. Statistics analysis

R studio was used to perform LASSO, in order to get the predictive radiomics features. The LASSO cox proportional hazards regression was performed to establish radiomics signature model. Clinical information and image semantic features were added to construct combined model. SPSS (IBM Corporation: Armonk, NY) 19.0 software was used to analysis the index. If they were normal distribution, we used Student's *t*-test, otherwise we used Mann-Whitney *U* test to find statistic significant. If *P* value less than .05, it was considered statistically significant.

3. Results

3.1. Characteristics of the patients

Total of 181 cases were randomly divided into train group and validation group by computer. The characteristics of the patients are presented in Tables 1 and 2, and there was no significant difference in variables between the 2 groups. The basic characteristics of the 2 groups of patients are as follows. The B hepatitis were 124 cases, C hepatitis were 19 cases. Alcoholic hepatitis were 6 cases. Mix type (B and C or B and alcoholic or C and alcoholic) were 14 cases, and others were 18 cases. Class I of

Table 1
The characteristics of the patients.

Variables		Train	Validation	P
Gender	Male	99 (83.2%)	47 (75.8%)	.232
	Female	20 (16.8%)	15 (24.2%)	
TNM	Stage I	101 (84.9%)	51 (82.3%)	.649
	Stage II	18 (15.1%)	11 (17.7%)	
Differentiation	Low	21 (17.6%)	18 (29.0%)	.077
	Others	98 (82.4%)	44 (71.0%)	
Age (yr)		58.48 ± 11.23	56.74 ± 9.93	.266
ALT (U/L)		32.70	38.05	.519
AST (U/L)		35.00	38.50	.267
AFP (ng/mL)		15.17	19.96	.086
PLT (e + 12)		117.00	112.00	.881

AFP = alpha-fetoprotein, ALT = alanine aminotransferase, AST = aspartate aminotransferase, PLT = platelet, TNM = tumor-node-metastasis.

Table 2
The characteristics of radiology.

Radiology trails	Total	Train	Validation	P
Lesions				
Lesion number = 1	126 (69.6%)	83 (69.7%)	43 (69.4%)	.956
Lesion number > 1	55 (30.4%)	36 (30.3%)	19 (30.6%)	
Artery supply				
Present = 1	67 (37%)	42 (35.3%)	25 (40.3%)	.506
Absent = 0	114 (63%)	77 (64.7%)	37 (59.7%)	
Capsule				
Present = 1	52 (28.7%)	38 (31.9%)	14 (22.6%)	.187
Absent = 0	129 (71.3%)	81 (68.1%)	48 (77.4%)	
Margin clear				
Yes = 0	142 (78.5%)	89 (74.8%)	53 (85.5%)	.097
No = 1	39 (21.5%)	30 (25.2%)	9 (14.5%)	
Enhancement				
Homogeneous = 0	41 (22.7%)	29 (24.4%)	12 (19.4%)	.444
Heterogeneous = 1	140 (77.3%)	90 (75.6%)	50 (80.6%)	
Necrosis				
Present = 1	67 (37%)	43 (36.1%)	24 (38.7%)	.733
Absent = 0	114 (63%)	76 (63.9%)	38 (61.3%)	
TNM				
I stage = 1	152 (84%)	101 (84.9%)	51 (82.3%)	.649
II stage = 2	29 (16%)	18 (15.1%)	11 (17.7%)	
Differentiation				
Low = 1	39 (21.5%)	21 (17.6%)	18 (29%)	.077
Others = 2	142 (78.5%)	98 (82.4%)	44 (71%)	

Low = low differentiation, TNM = tumor-node-metastasis.

tumor node metastasis stage were 152 cases, and class II were 29 cases. Low differentiation of pathology type were 39 cases, and others were 142 cases. As shown in Table 2, there were no significant differences in radiological characteristics between the 2 groups.

The mean time of recurrence in the train and validation group were 10.53 (3.6–33.1) months and 12.13 (4.76–29.28) months, and the mean follow-up time were 45.17 (25.00–57.67) months and 41.50 (24.42–61.50) months, respectively. There were 94 cases of recurrence at 1 year, 26 cases at 2 years, 14 cases at 3 years, and 47 cases without recurrence.

3.2. Feature selection of radiomics and development of the rad-score

The LASSO cox proportional hazards regression was used to reduce the dimensionality of the above high-dimensional features based on the optimal λ parameters, and the features with highly relevant were screened (Figs. 1 and 2). There were 4 out of 34 radiomic features selected, including T1.HISTO_Kurtosis,

T1.SHAPE_Sphericity, T1.SHAPE_Compacity, and T1.NGLDM_Contrast. The rad-score calculation formula consisting of these features. The optimal cutoff for rad-score was -0.76. Patients were divided into high (>-0.76) and low (≤-0.76) groups according to the rad-score. Patients with high rad-score were positively associated with early recurrence, suggesting that high rad-score may indicate tumor early recurrence (Fig. 3). The LASSO Cox proportional hazards regression was used to construct radiomic model.

Rad-score = 0.7199 * SCOR + 0.5184 * Number + 0.4056 * capsule - 0.8551 * (Biopsy-1) + 0.3416 * log10 AFP.

3.3. The performance of predictive model

In this study, meaningful features for constructing predictions model included rad-score, number of lesions, capsule integrity, necrosis, age, gender, pathological type, AFP, and alanine transaminase. Multivariate analyses suggested that the rad-score, number of lesions, integrity of the capsule, biopsy result, and AFP were independent influencing factors (Tables 3 and 4).

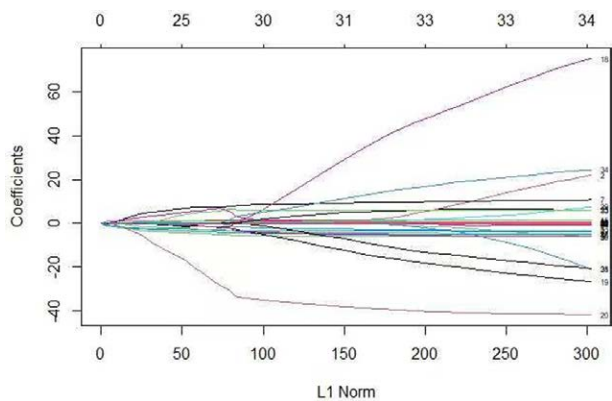


Figure 1. LASSO regression coefficients. LASSO = least absolute shrinkage and selection operator.

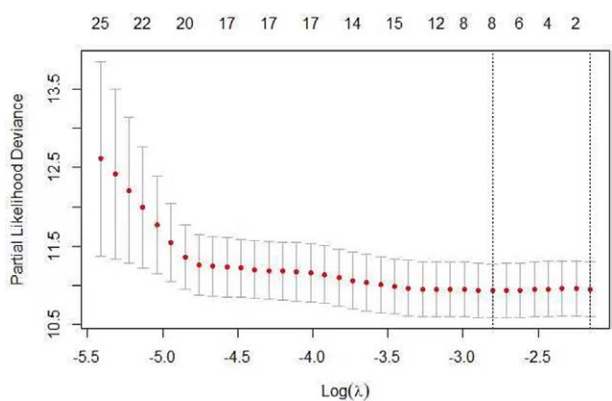


Figure 2. Cross validation plot for the penalty term.

Based on the results of multivariate analysis, rad-score based nomogram predicting recurrence of HCC after ablation, as showed in Figure 4. In the nomogram, each factor was ascribed

a weighted point that implied a risk of recurrence or survival. The calibration curve shows the excellent prediction accuracy of the model predicting the recurrence in the train and validation groups (Fig. 5a–f).

The C-index of the train group and validation group was 0.72 (95% CI: 0.66, 0.78) and 0.71 (95% CI: 0.67, 0.76), respectively. The area under the curve of predicting early recurrence at 1, 2, and 3 years in the train group was 0.79 (95% CI: 0.72–0.88), 0.72 (95% CI: 0.63–0.82), and 0.71 (95% CI: 0.61–0.83) (Fig. 6a), respectively. The result of the validation group was 0.72 (1 year) (95% CI: 0.58–0.84), 0.61 (2 years) (95% CI: 0.45–0.78) and 0.64 (3 years) (95% CI: 0.40–0.87) (Fig. 6b), respectively. The performance of the predictive model is showed in Tables 5 and 6. Evaluation indicators include precision, accuracy, sensitivity, specificity, positive predictive value, and negative predictive value.

4. Discussion

There are still challenges to effectively predicting early recurrence after HCC ablation. In the present study, we constructed a predictive integrated model which was the combination of clinical data, imaging and radiomics features. We used MRI-based radiomics because it might powerful in detecting tumor heterogeneity compared to CT, however, lacked further quantitative data. Therefore, radiomics of MRI combined with CT maybe improve the model's effectiveness. The integrated model presented good predictive performance, suggesting that early HCC recurrence after ablation required multidimensional markers of clinical and radiography. This result was in accordance with previous studies.^[24–26]

First-order features quantitatively delineate the distribution of voxel intensities within the image through fundamental metrics, such as features of histogram and shape-based. The histogram is frequency distribution of pixel/voxel gray values without considering their spatial orientation. Tumor intensity histogram-based features reduce the 3D data of a tumor volume into a single histogram. This histogram describes the fractional volume for a selected structure for the range of voxel values.^[16] Shape-based features present the morphological structure of the lesion.^[27] It shows how the tumor is nearly spherical, round,

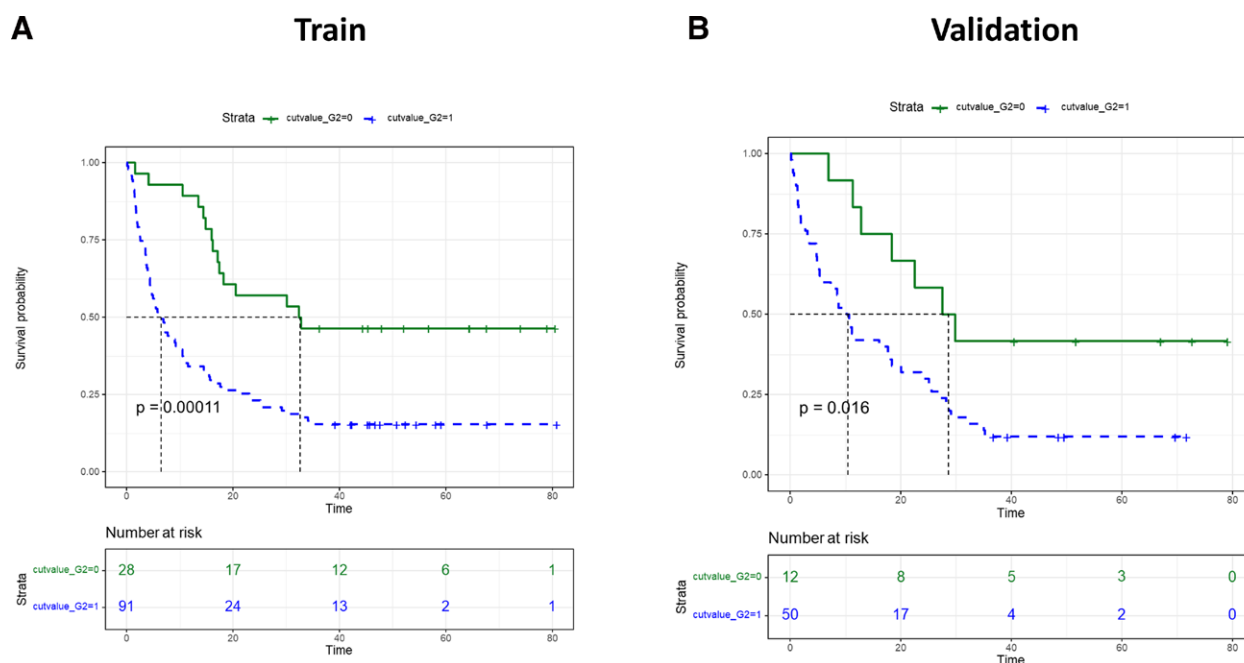


Figure 3. Prognostic significance of rad-score for patients of HCC after ablation. HCC = hepatocellular carcinoma.

Table 3
Univariate logistic regression analysis of radiological and clinical features.

Variables	HR	95% CI	P
Rad-score	1.42	1.06–1.90	.0196*
Number of lesions	2.97	1.39–6.36	.0050*
Artery supply	1.33	0.76–2.33	.3127
Capsule	2.63	1.34–5.18	.0052*
Margin clear	1.44	0.75–2.76	.2693
Uniform	1.01	0.48–2.14	.9821
Necrosis	1.80	0.94–3.44	.0745
Age	1.25	0.86–1.83	.2457
Gender	0.48	0.20–1.14	.0950
TNM	0.58	0.24–1.40	.2260
Low differentiation	0.44	0.21–0.90	.0253*
AFP	1.59	1.10–2.30	.0135*
PLT	1.01	0.68–1.51	.9641
AST	1.00	0.54–1.86	.9999
ALT	1.65	0.90–3.01	.1049

AFP = alpha-fetoprotein, ALT = alanine aminotransferase, AST = aspartate aminotransferase, PLT = platelet, TNM = tumor-node-metastasis.
* represents significant differences.

or elongated in shape. Quantitative features describe the geometric shape of a tumor, and could also be extracted from the 3D surface of the rendered volumes. Tumors that were more spherical were less likely to have early recurrence, this was consistent with previous research.^[12] Lesions that were not nearly spherical probably indicated microvascular invasion, suggesting early recurrence.^[28] Density means that the denser the tumor, the higher the heterogeneity and suggests a worse prognosis. Kurtosis is the peak of the region of interest pixel distribution, which could be used to describe the concentration degree of

Table 4
Multivariate logistic regression analysis of radiological and clinical features.

Variables	HR	95% CI	P
Rad-score	1.45	1.09–1.93	.0098*
Number of lesions	2.27	1.28–4.02	.0048*
Capsule	2.67	1.46–4.89	.0015*
Necrosis	1.81	0.99–3.28	.0529
Gender	0.56	0.25–1.28	.1690
Differentiation	0.36	0.18–0.70	.0028*
AFP	1.68	1.21–2.32	.0018*
ALT	1.50	1.12–2.01	.0059

AFP = alpha-fetoprotein, ALT = alanine aminotransferase.
* represents significant differences.

image brightness information. A higher kurtosis implies that the mass of the distribution is concentrated towards the tail rather than that towards the mean.^[8,29] In the present study, we outlined every slice of the whole tumor. Although this work took time, more radiomics features were obtained. These works improved the credibility of the research and the accuracy of the results. It is probably more precise than studies that only measure the largest dimension of the tumor.^[30] At present, many radiomics studies on HCC had used CT images as the main data.^[31] However, in this study, we applied MRI images to extract radiomics features and constructed the prediction model for the early recurrence of HCC.

Radiological features are an important part of tumor research. In the present study, we recorded imaging characteristics to build the integrated model such as margin, artery supply, capsule, and necrosis. Some of them were proven independent factors for the prognosis of HCC.^[32,33] The previous study

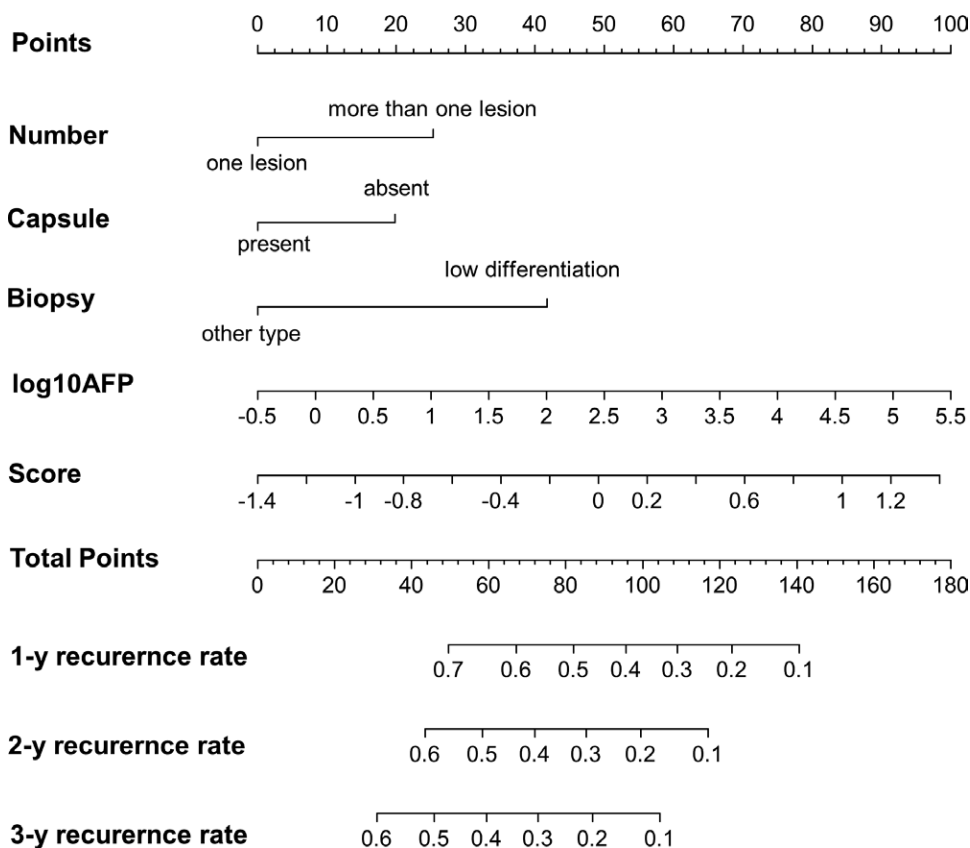


Figure 4. The prognostic nomogram for recurrence.

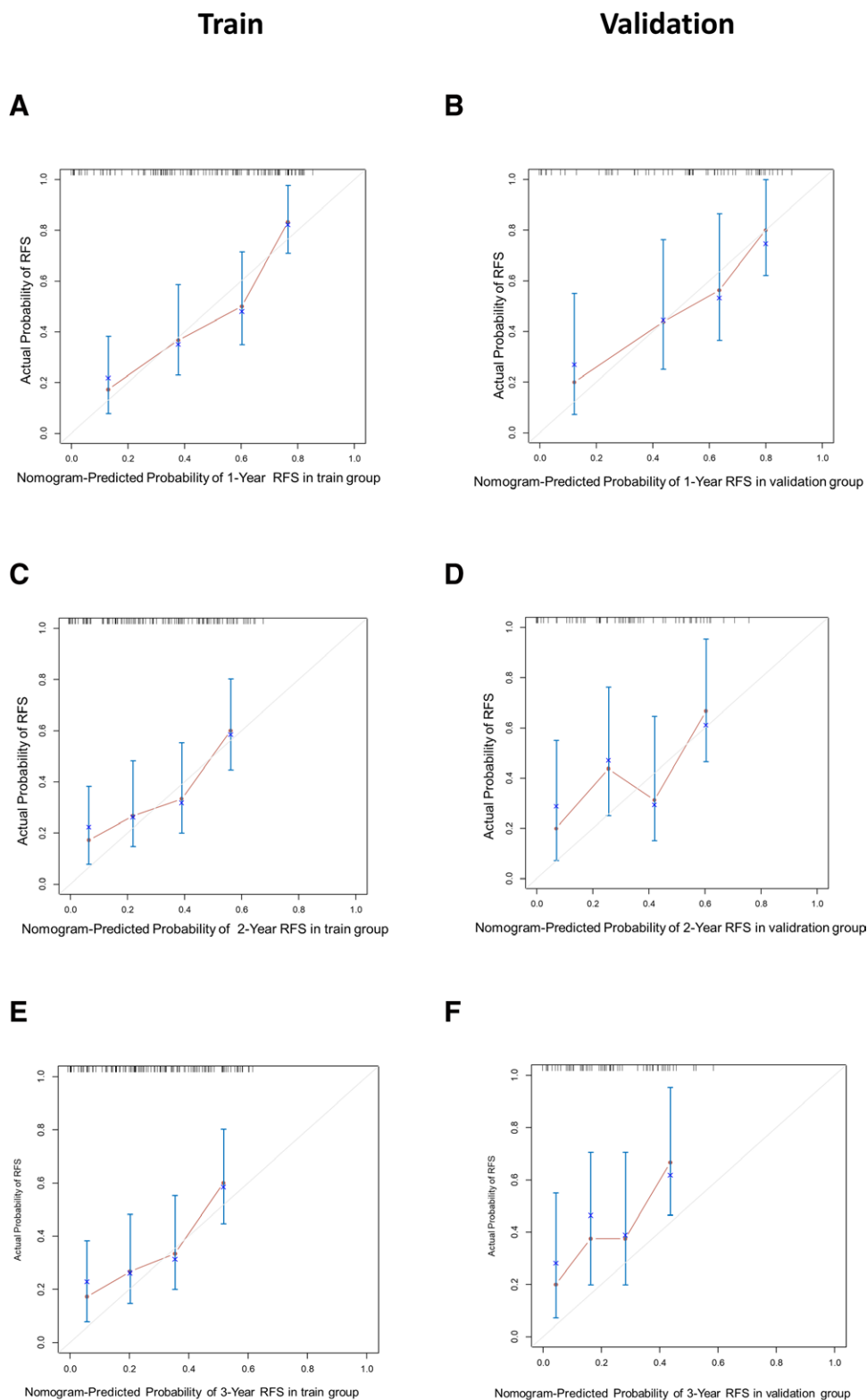


Figure 5. Calibration curves of the nomogram for recurrence.

showed that the integrity of the capsule was an independent factor for prognosis.^[34] However, patients in that study were treated with hepatectomy, not after ablation. The radiological features were relative with tumor heterogeneity. In the present study, results showed that the integrity of the capsule is the only one that was relative to early recurrence. Meanwhile, when the capsule was integral, it was easy to make sure of the ablation

margin. Clear ablation margins are critical to treatment success. Encapsulated lesions are more likely to make clear the borders of ablation and margins extending to the periphery to prevent recurrence. In addition, if the tumor border is un-capsulated or not smooth, with feeding arteries and surrounding dark areas, these imaging features may suggest microvascular invasion, leading to early recurrence.^[2] The previous study also proved

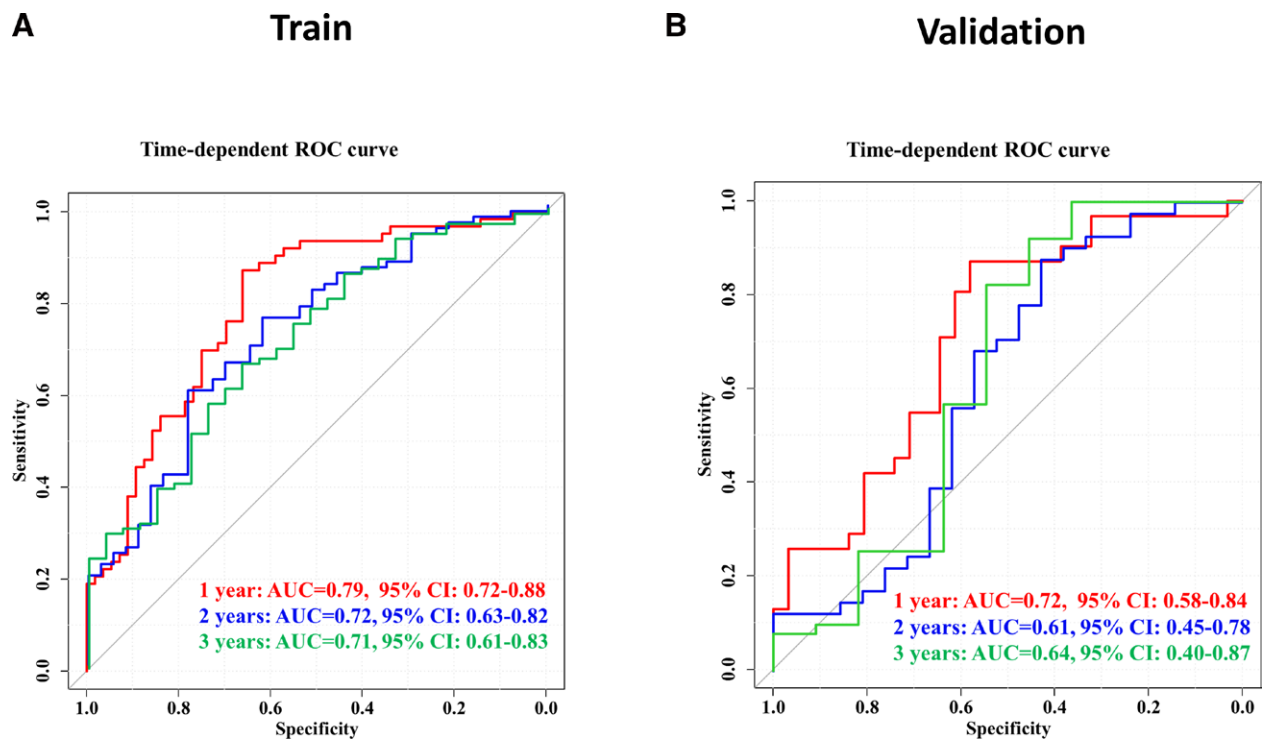


Figure 6. ROC curves. ROC = receiver operating characteristic curve.

Table 5

The performance of train group.

	Precision	Accuracy	Sensitivity	Specificity	PPV	NPV
1 yr	0.74	0.77	0.87	0.66	0.74	0.82
2 yr	0.86	0.66	0.60	0.78	0.86	0.47
3 yr	0.87	0.66	0.66	0.67	0.87	0.37

NPV = negative predictive value, PPV = positive predictive value.

Table 6

The performance of validation group.

	Precision	Accuracy	Sensitivity	Specificity	PPV	NPV
1 yr	0.66	0.73	0.87	0.58	0.68	0.82
2 yr	0.75	0.73	0.88	0.43	0.75	0.64
3 yr	0.89	0.84	0.92	0.45	0.89	0.56

NPV = negative predictive value, PPV = positive predictive value.

that the non-smooth tumor margin was a significant predictor for early recurrence.^[14]

In the present study, 4 radiomics features were selected by LASSO, they were T1. HISTO_Kurtosis, T1. SHAPE_Sphericity, T1. SHAPE_Compacity, and T1. NGLDM_Contrast. We investigated 5 different series images, for more details of the image would be gained from different phases and series. But some studies had investigated partial series.^[35] After analysis, the meaningful features of radiomics obtained were all derived from T1WI. T1WI could show the characteristics of tissue anatomy well. SHAPE_Sphericity showed the characteristic of the lesion being close to spherical. Sphericity was equal to 1 for a perfect sphere. The previous study suggested that non-smooth tumor margins predict early recurrence of single HCC.^[36] Ablation

would be well performed when the tumorous margin was regular and smooth. The electrode needle forms a spherical area of ablation, covering the tumor and its surrounding margin so that the tumor tends to be cured. Clinically, patients with lesions that are aspheric, multiple, non-encapsulated, poorly differentiated, and high in alpha-fetoprotein value, should be followed up strictly. Combined therapy should be performed as soon as possible, such as targeted and immunotherapy, traditional Chinese medicine, radiotherapy and other combined therapy. SHAPE_Compacity reflected how compact the VOI was. The radiomic feature may relative with the amount of hepatocellular carcinoma. During ablation, power and treatment time are both important factors in the success of the operation. For patients with early recurrence, it may be necessary to increase

the power or prolong the treatment time. In addition, compared with enhanced MRI, plain MRI is more economical and saves examination time. This is very beneficial for patients with renal failure or for whom enhanced MRI is contraindicated. As far as we know, although some studies suggested that the portal venous phase or series of DWI were meaningful for the prognosis of HCC,^[37] only this study was based on ablation therapy until now. T1WI could well present tissue anatomy, and most of the radiomics features are related to spatial distribution, such as shape and histogram. In addition, NGLDM_Contrast is the intensity difference between neighboring regions. Spatial distribution of pixel/voxel gray levels in relation to their relative positions. In the present study, the radiomics feature, NGLDM_Contrast, was related to the gray level intensity variation of the pixels that make up the tumor image.

The present study still has some limitations. Research data was limited, and this was a retrospective study. The study data came from our own institution. The multiple centers, prospective study with more samples will be needed in the future. It was suggested that the peritumor segmentation could better predict recurrence. DWI series is important for HCC prognosis. However, some of the lesions in the present study were too small to segmentation. We aim to made some effort to prove it further.

5. Conclusions

We established a predictive integrated model for early recurrence of HCC after ablation, and the model presented good predictive performance. For the early recurrence patient, the individual medicine was required.

Author contributions

Conceptualization: Zhenchang Wang.

Data curation: Xiaozhen Yang.

Formal analysis: Xiaozhen Yang, Chunwang Yuan.

Investigation: Yinghua Zhang, Kang Li.

Writing – original draft: Xiaozhen Yang, Chunwang Yuan, Yinghua Zhang, Kang Li, Zhenchang Wang.

Writing – review & editing: Xiaozhen Yang, Chunwang Yuan, Yinghua Zhang, Kang Li, Zhenchang Wang.

References

- [1] Peter RG, Alejandro F, Josep ML, et al. European Association for the Study of the Liver. Electronic address EEE, European association for the study of the L. EASL clinical practice guidelines: management of hepatocellular carcinoma. *J Hepatol.* 2018;69:182–236.
- [2] Peng J, Zhang J, Zhang Q, et al. A radiomics nomogram for preoperative prediction of microvascular invasion risk in hepatitis B virus-related hepatocellular carcinoma. *Diagn Interv Radiol.* 2018;24:121–7.
- [3] Zheng J, Chakraborty J, Chapman WC, et al. Preoperative prediction of microvascular invasion in hepatocellular carcinoma using quantitative image analysis. *J Am Coll Surg.* 2017;225:778–788e1.
- [4] Hui TCH, Chuah TK, Low HM, et al. Predicting early recurrence of hepatocellular carcinoma with texture analysis of preoperative MRI: a radiomics study. *Clin Radiol.* 2018;73:1056.e111056 e11–1056.e16.
- [5] Silva M, Mattos AA, Fontes PR, et al. [Evaluation of hepatic resection for hepatocellular carcinoma on cirrhotic livers] avaliacao da ressecao hepatica em pacientes cirroticos com carcinoma hepatocelular. *Arq Gastroenterol.* 2008;45:99–105.
- [6] Zhang W, Lai SL, Chen J, et al. Validated preoperative computed tomography risk estimation for postoperative hepatocellular carcinoma recurrence. *World J Gastroenterol.* 2017;23:6467–73.
- [7] Ahn SJ, Kim JH, Park SJ, et al. Hepatocellular carcinoma: preoperative gadoxetic acid-enhanced MR imaging can predict early recurrence after curative resection using image features and texture analysis. *Abdom Radiol.* 2019;44:539–48.
- [8] Feng ST, Jia Y, Liao B, et al. Preoperative prediction of microvascular invasion in hepatocellular cancer: a radiomics model using Gd-EOB-DTPA-enhanced MRI. *Eur Radiol.* 2019;29:4648–59.

- [9] Liu Z, Wang S, Dong D, et al. The applications of radiomics in precision diagnosis and treatment of oncology: opportunities and challenges. *Theranostics.* 2019;9:1303–22.
- [10] Lambin P, Rios-Velazquez E, Leijenaar R, et al. Radiomics: extracting more information from medical images using advanced feature analysis. *Eur J Cancer.* 2012;48:441–6.
- [11] Zheng BH, Liu LZ, Zhang ZZ, et al. Radiomics score: a potential prognostic imaging feature for postoperative survival of solitary HCC patients. *BMC Cancer.* 2018;18:1148.
- [12] Chen S, Zhu Y, Liu Z, et al. Texture analysis of baseline multiphase hepatic computed tomography images for the prognosis of single hepatocellular carcinoma after hepatectomy: a retrospective pilot study. *Eur J Radiol.* 2017;90:198–204.
- [13] Simpson AL, Adams LB, Allen PJ, et al. Texture analysis of preoperative CT images for prediction of postoperative hepatic insufficiency: a preliminary study. *J Am Coll Surg.* 2015;220:339–46.
- [14] Zhang Z, Jiang H, Chen J, et al. Hepatocellular carcinoma: radiomics nomogram on gadoxetic acid-enhanced MR imaging for early postoperative recurrence prediction. *Cancer Imag.* 2019;19:22.
- [15] Cozzi L, Dinapoli N, Fogliata A, et al. Radiomics based analysis to predict local control and survival in hepatocellular carcinoma patients treated with volumetric modulated arc therapy. *BMC Cancer.* 2017;17:829.
- [16] Li Z, Mao Y, Huang W, et al. Texture-based classification of different single liver lesion based on SPAIR T2W MRI images. *BMC Med Imaging.* 2017;17:42.
- [17] Yu K, Zhang Y, Yu Y, et al. Radiomic analysis in prediction of human papilloma virus status. *Clini Transl Rad Oncol.* 2017;7:49–54.
- [18] Ferreira Junior JR, Koenigkam-Santos M, Cipriano FEG, et al. Radiomics-based features for pattern recognition of lung cancer histopathology and metastases. *Comput Methods Programs Biomed.* 2018;159:23–30.
- [19] Shi L, He Y, Yuan Z, et al. Radiomics for response and outcome assessment for non-small cell lung cancer. *Technol Cancer Res Treatment.* 2018;17:1533033818782788.
- [20] Huang X, Long L, Wei J, et al. Radiomics for diagnosis of dual-phenotype hepatocellular carcinoma using Gd-EOB-DTPA-enhanced MRI and patient prognosis. *J Cancer Res Clin Oncol.* 2019;145:2995–3003.
- [21] Rahmim A, Huang P, Shenkov N, et al. Improved prediction of outcome in Parkinson's disease using radiomics analysis of longitudinal DAT SPECT images. *NeuroImage Clinical.* 2017;16:539–44.
- [22] van Velden FH, Kramer GM, Frings V, et al. Repeatability of radiomic features in non-small-cell lung cancer [(18)F]FDG-PET/CT studies: impact of reconstruction and delineation. *Mol Imaging Biol.* 2016;18:788–95.
- [23] Wakabayashi T, Ouhmich F, Gonzalez-Cabrera C, et al. Radiomics in hepatocellular carcinoma: a quantitative review. *Hepatol Int.* 2019;13:546–59.
- [24] Cai W, He B, Hu M, et al. A radiomics-based nomogram for the preoperative prediction of posthepatectomy liver failure in patients with hepatocellular carcinoma. *Surg Oncol.* 2019;28:78–85.
- [25] Zhou H, Dong D, Chen B, et al. Diagnosis of distant metastasis of lung cancer: based on clinical and radiomic features. *Transl Oncol.* 2018;11:31–6.
- [26] Zhao Y, Wu J, Zhang Q, et al. Radiomics analysis based on multiparametric MRI for predicting early recurrence in hepatocellular carcinoma after partial hepatectomy. *J Magn Reson Imaging.* 2021;53:1066–79.
- [27] Mule S, Thieffn G, Costentin C, et al. Advanced hepatocellular carcinoma: pretreatment contrast-enhanced CT texture parameters as predictive biomarkers of survival in patients treated with Sorafenib. *Radiology.* 2018;288:445–55.
- [28] Yang L, Gu D, Wei J, et al. A radiomics nomogram for preoperative prediction of microvascular invasion in hepatocellular carcinoma. *Liver Cancer.* 2019;8:373–86.
- [29] Yu JY, Zhang HP, Tang ZY, et al. Value of texture analysis based on enhanced MRI for predicting an early therapeutic response to transcatheter arterial chemoembolisation combined with high-intensity focused ultrasound treatment in hepatocellular carcinoma. *Clin Radiol.* 2018;73:758.e9758 e9–758.e18.
- [30] Ng F, Kozarski R, Ganeshan B, et al. Assessment of tumor heterogeneity by CT texture analysis: can the largest cross-sectional area be used as an alternative to whole tumor analysis?. *Eur J Radiol.* 2013;82:342–8.
- [31] Wei J, Jiang H, Gu D, et al. Radiomics in liver diseases: current progress and future opportunities. *Liver Int.* 2020;40:2050–63.

- [32] Oh J, Lee JM, Park J, et al. Hepatocellular carcinoma: texture analysis of preoperative computed tomography images can provide markers of tumor grade and disease-free survival. *Korean J Radiol.* 2019;20:569–79.
- [33] Zhang J, Liu X, Zhang H, et al. Texture analysis based on preoperative magnetic resonance imaging (MRI) and conventional MRI features for predicting the early recurrence of single hepatocellular carcinoma after hepatectomy. *Acad Radiol.* 2019;26:1164–73.
- [34] Horvat N, Monti S, Oliveira BC, et al. State of the art in magnetic resonance imaging of hepatocellular carcinoma. *Radiol Oncol.* 2018;52:353–64.
- [35] Liu X, Li Y, Qian Z, et al. A radiomic signature as a non-invasive predictor of progression-free survival in patients with lower-grade gliomas. *NeuroImage Clin.* 2018;20:1070–7.
- [36] Lee S, Kim SH, Lee JE, et al. Preoperative gadoxetic acid-enhanced MRI for predicting microvascular invasion in patients with single hepatocellular carcinoma. *J Hepatol.* 2017;67:526–34.
- [37] Stocker D, Marquez HP, Wagner MW, et al. MRI texture analysis for differentiation of malignant and benign hepatocellular tumors in the non-cirrhotic liver. *Heliyon.* 2018;4:e00987.